NUMERICAL SIMULATION OF FLOW IN THERMAL PLASMA TORCH UNDER DIFFERENT OPERATING CONDITIONS

Celso Luiz Felipini, celsofelipini@gmail.com
Universidade São Judas Tadeu, Rua Taquari 546, São Paulo, 03116-000, Brazil
Universidade de São Paulo, Av. Prof. Mello Moraes 2231, São Paulo, 05508-900, Brazil
Marcos de Mattos Pimenta, marcos.pimenta@poli.usp.br
Universidade de São Paulo, Av. Prof. Mello Moraes 2231, São Paulo, 05508-900, Brazil

Abstract. *The main purpose of this article is to present and discuss the results of numerical simulation of flow in a d.c. thermal plasma torch under different operating conditions. The mathematical model (magnetohydrodynamic model) and computer code (based on the Finite Volume Method) developed for the simulations are also concisely presented. A previous article presented the comparison of some numerical simulation results with literature and showed good agreement in most of the computational domain regions. The numerical simulation results presented in this article were obtained for case studies with different operating conditions. Such results allowed us to verify the effects of these conditions on the behavior of temperature and axial velocity profiles of the plasma flow. The simulated operating conditions were: gas flow rate (5, 10 and 15l/min); electric current intensity (100A and 200A); plasmogenic gases (air and argon). The results showed that the developed model is suitable for obtaining a better understanding of the involved phenomena (interaction arc/flow) and it is also useful for the optimization of torches.*

Keywords*: Thermal plasma, Plasma torch, MHD model, Numerical simulation, Finite volume method*

1. INTRODUCTION

Over the past four decades, the technology of thermal plasma has been widely applied to several industrial mechanical, metallurgical and chemical processes (Boulos et al., 1994; Fauchais and Vardelle, 2000; Pfender, 2000; Gomez et al., 2009; Rao et al., 2013). The main features that make thermal plasmas technologically attractive are: high energy density (that comes with high heat flux density), high quenching rate, high processing rates and relatively small installation sizes (Pfender, 1978; Solonenko and Zhukov, 1995; Trelles et al., 2009).

Direct current (*DC*) arc thermal plasma torches are devices designed to generate plasma jets of high enthalpies, high temperatures and high velocities, from *DC* electrical power conversion (Venkatramani, 2002). These devices are involved in many applications such as: atmospheric pressure plasma spraying, plasma-assisted chemical vapor deposition, plasma preparation of ultra-fine powders, production of high purity metals and nanomaterials, thermal plasma waste treatment. Several reviews of these applications have been presented in literature: Pfender (2000), Venkatramani (2002), Fauchais (2004), Heberlein and Murphy (2008), Gomez et al. (2009), Mihovsky (2010), Abdulkarim and Hassan (2015) and Vardelle et al. (2015).

Thermal plasma torch designs using electric arc (usually called plasma torches) should be specifically developed according to their applications (Feinman, 1987). Therefore, the optimization of electrothermic processes involving thermal plasmas is closely related to the proper conception of plasma torches, mainly concerning to geometry/dimensions of electrodes (anodes and cathodes) and to operating parameters: working gas (plasmogenic gas), electric current intensity, electric voltage, gas flow rate and temperature range (Boulos et al., 1994). Besides the experimental procedures used in the development of plasma torches, the Computational Fluid Dynamics (*CFD*) is an interesting tool for torch design and optimization because it allows reducing the development costs and it helps to understand the related phenomena (Solonenko and Zhukov, 1995; Gleizes et al., 2005; Trelles et al., 2009).

The model of this work refers to non-transferred arc torches (torches where the electric circuit closes among electrodes, cathodes and anodes, inside the torches themselves and the plasma jet does not conduct the current to their outer part), specifically the ones destined to industrial applications (thermal spraying, etc.) and the solutions for waste, contaminated residues, toxic material and pollutants which affect the environment (Fig. 1).

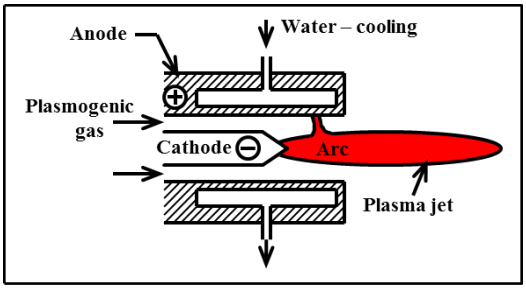

Figure 1. Schematic representation of a non-transferred arc plasma torch.

This article presents and discusses the results of numerical simulation of flow in a *DC* thermal plasma torch under different operating conditions. The mathematical model and computer code developed for the simulations are also concisely presented. A previous article (Felipini and Pimenta, 2015) presented the comparison of some numerical simulation results with literature and showed good agreement in most of the computational domain regions: the biggest difference between experimental temperature values and calculated values was -10%, and the average of the differences obtained in the comparisons was approximately ±3,2%.

2. MODEL DESCRIPTION

A magnetohydrodynamic model (*MHD* model) was adapted to thermal plasma torches based on Scott et al. (1989), Westhoff and Szekely (1991), Murphy and Kovitya (1993), Bauchire et al. (1997), Favalli (1997), Bianchini (2000), Klinger (2002), Baudry (2003), Li et al. (2003), Yuan et al. (2004), Gleizes, et al. (2005), Li and Pfender (2007), Trelles et al. (2009) and Huang et al. (2013). Its main characteristics are: two dimensional mathematical model (axisymmetric) of swirling flow in non-transferred arc thermal plasma torches which operate in *DC*, involving all regions of study interest and influence in phenomena (gas inlet; inside torch– where there is arc/flow interaction; plasma jet free in the environment).

In this article, the mathematical model and computer code developed for the simulations are concisely presented. A more detailed description is presented in Felipini (2015).

The following assumptions have been adopted for this model: (1) plasma (electrons; heavy particles) has a *Newtonian* and single-species fluid behavior; (2) flow is approached in a continuum, two dimensional (axisymmetric), laminar, and steady state; (3) the local thermodynamic equilibrium (*LTE*) prevails in the study domain; (4) plasma is optically thin (black body radiation emitted by plasma is not absorbed by it); (5) heat dissipation due to viscous tensions may not be taken into consideration (constituted by second order terms); (6) *MHD* approach is applicable: displacement current is not considered when compared to the conduction current; the electrostatic field strength is not considered; (7) gravity effects are not considered; (8) the external environment is formed by the same gas as the work one.

By taking into consideration the assumptions previously adopted, the governing equations for the axisymmetric (*2D*), laminar flow in stationary status with plasma torch swirl may be presented in cylindrical coordinates as follows:

Mass conservation equation:

$$\frac{1}{r}\frac{\partial}{\partial r}(r\rho v)+\frac{\partial}{\partial z}(\rho u)=0 \tag{1}$$

Momentum conservation equations in z (axial), r (radial) and θ (azimuthal) directions, respectively:

$$\frac{1}{r}\frac{\partial}{\partial r}(r\rho uv)+\frac{\partial}{\partial z}\left(\rho u^2\right)=\frac{1}{r}\frac{\partial}{\partial r}\left[r\mu\left(\frac{\partial u}{\partial r}+\frac{\partial v}{\partial z}\right)\right]+\frac{\partial}{\partial z}\left(2\mu\frac{\partial u}{\partial z}\right)-\frac{\partial p}{\partial z}+j_r B_\theta \tag{2}$$

$$\frac{1}{r}\frac{\partial}{\partial r}\left(r\rho v^2\right)+\frac{\partial}{\partial z}(\rho uv)=\frac{1}{r}\frac{\partial}{\partial r}\left(2r\mu\frac{\partial v}{\partial r}\right)+\frac{\partial}{\partial z}\left[\mu\left(\frac{\partial u}{\partial r}+\frac{\partial v}{\partial z}\right)\right]+\rho\frac{w^2}{r}-2\mu\frac{v}{r^2}-\frac{\partial p}{\partial r}-j_z B_\theta \tag{3}$$

$$\frac{1}{r}\frac{\partial}{\partial r}(r\rho vw)+\frac{\partial}{\partial z}(\rho uw)=\frac{1}{r}\frac{\partial}{\partial r}\left(r\mu\frac{\partial w}{\partial r}\right)+\frac{\partial}{\partial z}\left(\mu\frac{\partial w}{\partial z}\right)-\frac{1}{r^2}\mu w-\rho\frac{vw}{r} \tag{4}$$

where u, v and w are the velocity components in z (axial), r (radial) and θ (azimuthal) directions, respectively; μ, ρ and p are the following gas properties: dynamic viscosity, specific mass and pressure, respectively; j_z and j_r are the axial and radial components of the electric current density vector $\vec{j}$, respectively, and B_θ is the azimuthal component of the magnetic induction intensity vector (self-induced) $\vec{B}$ (note: "magnetic field inducted by the arc electric field"). Observe that $j_r B_\theta$ and $j_z B_\theta$ terms are components of *Lorentz* force vector: $\vec{F}$ ($\vec{F}=\vec{j}\times\vec{B}$).

Energy conservation equation ("written" in function of the gas specific enthalpy, h: $h=\int C_p dT$):

$$\frac{1}{r}\frac{\partial}{\partial r}(r\rho vh)+\frac{\partial}{\partial z}(\rho uh)=\frac{1}{r}\frac{\partial}{\partial r}\left(r\frac{k}{C_p}\frac{\partial h}{\partial r}\right)+\frac{\partial}{\partial z}\left(\frac{k}{C_p}\frac{\partial h}{\partial z}\right)+\frac{j_r^2+j_z^2}{\sigma}-S_r+\frac{5}{2}\frac{k_b}{e}\left(\frac{j_r}{C_p}\frac{\partial h}{\partial r}+\frac{j_z}{C_p}\frac{\partial h}{\partial z}\right)$$
$$+u\frac{\partial p}{\partial z}+v\frac{\partial p}{\partial r} \tag{5}$$

where C_p is the gas specific heat at constant pressure; k is the gas thermal conductivity and σ is the gas electrical conductivity. One should observe that besides the terms which represent the enthalpy transport through convection and diffusion, the energy conservation equation is constituted by the following source terms: $\frac{j_r^2 + j_z^2}{\sigma}$, heating through *Joule* effect; S_r, heat dissipation through radiation per unit of plasma volume ($S_r = 4\pi\varepsilon_N$, where ε_N is NEC emissivity - plasma is considered optically thin. Experimental values: Baudry (2003)); $\frac{5}{2}\frac{k_b}{e}\left(\frac{j_r}{C_p}\frac{\partial h}{\partial r} + \frac{j_z}{C_p}\frac{\partial h}{\partial z}\right)$ (*electron drift*) is the enthalpy transport through electron current which is directed to the anode (k_b is *Boltzmann* constant; e is the elementary electric charge); $u\frac{\partial p}{\partial z} + v\frac{\partial p}{\partial r}$, is the energy variation due to pressure variation.

Boulos et al. (1994) presents the thermodynamic and plasma transport properties for some gases (air; argon; others).

The current densities and the azimuthal component of the magnetic field are obtained through the electric current conservation equation solution, and through the third *Maxwell* equation, with the help of the "adapted" *Richardson-Dushmann* equation (applicable for thermionic emission).

Electric current conservation equation (in the form of electric potential):

$$\frac{1}{r}\frac{\partial}{\partial r}\left(r\sigma\frac{\partial \Phi}{\partial r}\right) + \frac{\partial}{\partial z}\left(\sigma\frac{\partial \Phi}{\partial z}\right) = 0 \tag{6}$$

where Φ is the electric potential.

Third *Maxwell* equation (in differential form):

$$\frac{1}{r}\frac{\partial}{\partial r}(rB_\theta) = \mu_0 j_z \tag{7}$$

where μ_0 is the magnetic permeability in free space (vacuum).

One should observe that this equation is applicable only for symmetric current distributions (in this specific case, symmetry related to axis: axisymmetry).

The current density vector $\vec{j}$ is related to the electric field intensity vector $\vec{E}$, or to the electric potential Φ, by $\vec{j} = \sigma\vec{E} = -\sigma\nabla\phi$. So, for such case (2D model): $j_z = -\sigma\frac{\partial \Phi}{\partial z}$ and $j_r = -\sigma\frac{\partial \Phi}{\partial r}$.

The computational domain used for the simulations of this work is schematized in Fig. 2.

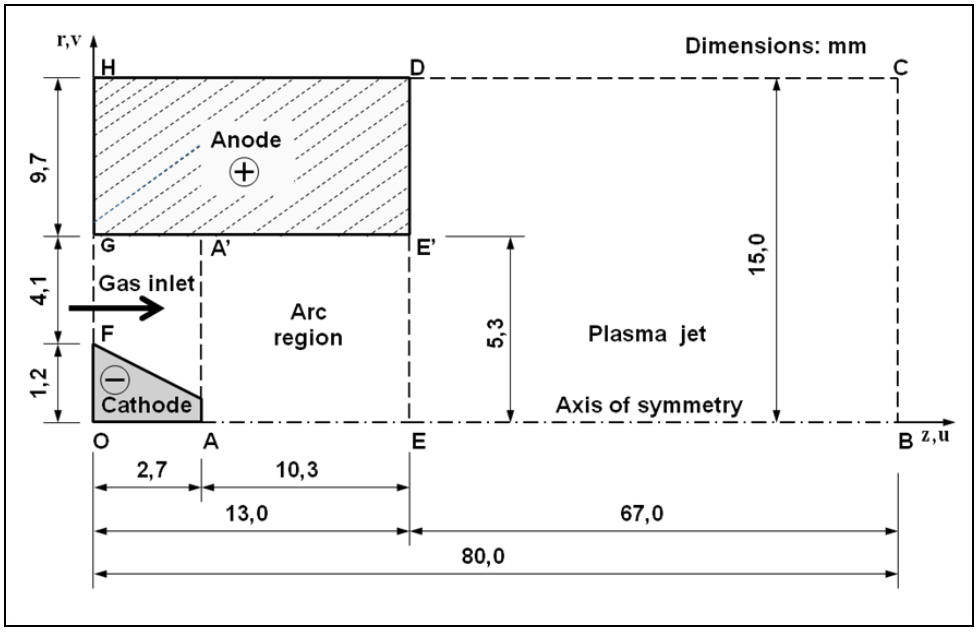

Figure 2. Computational domain.

The description of the employed boundary conditions is presented as follows:

Inlet (line *FG*): in the inlet section, the axial velocity presents a parabolic profile and depends on the specification of the gas flow rate. Radial velocity is zero at the inlet. Azimuthal velocity presents a profile partially formed by the behavior of free vortex and forced vortex. The azimuthal velocity depends on the swirl number in torch inlet. The definition of the swirl number (Sw) used in this model is presented by Westhoff and Szekely (1991).

It is emphasized that simulations in this work were performed with $w = 0$ and, therefore, $Sw = 0$ (flow without swirl).

Other conditions: on the surfaces of electrodes (anode and cathode), the *non-slip* conditions are assumed $(u = v = w = 0)$. In the symmetry axis (line *AB*): $\partial u / \partial r = 0$ and $v = w = 0$. Conditions of *free boundary* are assumed for *BC* and *CD*. For *BC*: $\partial(\rho u)/\partial z = 0$, $\partial v / \partial z = 0$ and $\partial w / \partial z = 0$. And for *CD*: $u = w = 0$ and $\partial(r\rho v)/\partial r = 0$. The boundary conditions for enthalpy are provided in temperature and converted to gas enthalpy. The temperature is 500K for the torch inlet, and 300 K for the line *CD*. The temperatures of cathode and anode surfaces are 3000K and 1000K, respectively. In the symmetry axis (line *AB*): $\partial h / \partial r = 0$; and in line *BC*, $\partial h / \partial z = 0$. Lines *AA'* and *EE'* are internal boundary conditions and are known as "fictitious" or "porous" boundary conditions (in these lines the boundary conditions for the electric potential (Φ) are assumed). In line *AA'*, the electric potential is determined by assuming a axial current density profile (Hsu et al., 1983; Murphy and Kovitya, 1993), adapted from *Richardson-Dushmann* equation (applicable for thermionic emission): $j_z(r) = j_0 e^{-r/r_c}$, where j_0 and r_c are constants which depend on the electric current and are experimentally obtained. In line *AB*: $\partial j_z / \partial r = 0$ and $j_r = 0$. In *ED*: $j_r = j_z = 0$. In anode: $\Phi = 0$.

Numerical method: the model was implemented in the *Computer Code for Simulation of the Swirling Flow in Thermal Plasma Torches* (*CTP*), developed in order to enable the numerical solution of governing equations. *CTP* code uses the *Finite Volume Method* (*FVM*) and it is based on (Vatavuk, 1996; Favalli, 1997; Bianchini, 2000). *CTP* was elaborated in *FORTRAN 90* language (*Microsoft FORTRAN Powerstation 4.0*) and the simulations were executed in a microcomputer with *INTEL CORE i7* processor and 6GB of *RAM* memory. The average computing time for each simulation is 15min, for meshes of 120x80 nodes and approximately 20000 iterations.

3. SIMULATION RESULTS AND COMMENTS

This section presents the results of some numerical simulations which were performed in order to verify whether the *CTP* code is suitable to simulate the effects of variations in operating conditions of plasma torches. Through simulations, it was also possible to verify whether the *CTP* is a useful tool to help understanding the phenomena related to the arc/flow interaction.

The methodology has been established as a case study based on the comparison of the effects caused by the variation of the following operating conditions of the torches: plasmogenic gas flow rate, electric current intensity and plasmogenic gas (argon; air). These conditions are critical to the development of torches for industrial and environmental applications.

The results obtained from the numerical simulations are presented in Fig. 3 to 8. In order to facilitate the comparison of the effects of different operating conditions, we opted for the presentation of the percentage differences of the physical quantities values (temperature and axial velocity) in positions of interest.

In some figures, the numerical values of physical quantities, percentage changes and their computational domain positions are also highlighted.

Comparisons of the temperature profiles for different gas flow rates (5, 10 and 15 l/min) (200A) are shown in Fig. 3 and comparisons of axial velocity profiles are shown in Fig. 4.

Figure 5 shows the comparisons of temperature profiles for different intensities of electric current (100A and 200A) and Fig. 6 shows the comparisons of axial velocity profiles.

Comparisons of the temperature profiles for different plasmogenic gases (argon and air) (200A) are shown in Fig. 7 and comparisons of axial velocity profiles are shown in Fig. 8.

Remarks related to the figures:

- All temperature and axial velocity profiles (as a function of axial distance) in this section (Fig. 3 to 8) refer to radial position: torch symmetry axis (r = 0);

- The directions of arrows in Fig. 3 mean: "up" indicates an increase of the temperature numerical value; "down" indicates a decrease of the temperature numerical value. Next to each arrow, the numerical value (in modulus) of increased or decreased temperature related to the value pointed out in the previous axial position is highlighted and the corresponding percentage value (in modulus) is presented between parentheses;

- Figures 3 and 4 show the differences (in modulus) of temperature or axial velocity between flow rates of 5 l/min (lowest flow rate) and 15 l/min (highest flow rate) for: maximum values; 13mm axial position; 80mm axial position. The percentage differences are also presented (in modulus) for the same flow rates and axial positions;

- In Fig. 5 to 8, the "negative sign" indicates the percentage increase between the compared values of the physical quantities (temperature and axial velocity) for different operating conditions, and the "positive sign" indicates a percentage decrease between the compared values;
- The percentage differences were calculated as follows:
  - (Figures 3 and 4): *dif%* = [(*V.G.*5 l/min – *V.G.*15 l/min) / *V.G.*5 lmin] x 100
    (results are presented in modulus)
  - (Figures 5 and 6): *dif%* = [(*V.G.*100A – *V.G.*200A) / *V.G.*100A] x 100
  - (Figures 7 and 8): *dif%* = [(*V.G.*argon – *V.G.*air) / *V.G.*argon] x 100

Where *V.G.*... "is the physical quantity value (temperature or axial velocity) for ... "

3.1 Case 1 - Gas flow rates: 5, 10 and 15 l/min

Analysis of Fig. 3 and 4 makes it possible to verify the following phenomenological characteristics:

In the region near the cathode (where there is maximum current density), due to gas ionization and, consequently, to its increased electrical conductivity, there is a big increase in the gas temperature due to its heating caused by *Joule* effect.

Still inside the torch (up to the distance *z*=13mm), there is a big decrease in plasma temperature due to the convection with the anode cooled surface. When the plasma jet comes out of the torch, it presents a smaller decrease of temperature, as a function of axial distance, due to the convection with the environmental gas. Also in the region near the cathode, there is plasma acceleration due to its expansion (caused by the temperature increase) and also due to *Lorentz* force effect (resulting from the interaction between the arc current and the inducted magnetic field). Then, there is a continuous deceleration of the velocity of plasma jet when in contact with the environmental gas.

Obviously, the quantitative results vary depending on different operating conditions of the torches, but qualitatively, it is emphasized that the characteristics of temperature and axial velocity profiles, obtained with the various simulations performed with the *CTP* code, are very similar to each other and they are also very similar to those reported in literature (for example: Westhoff and Szekely, 1991; Bauchire, et al., 1997).

In Fig. 3 it is possible to verify that the temperature profiles for the argon flow rate from 5 to 15 l/min practically coincide from torch inlet to axial distance of 5mm (inside the torch).

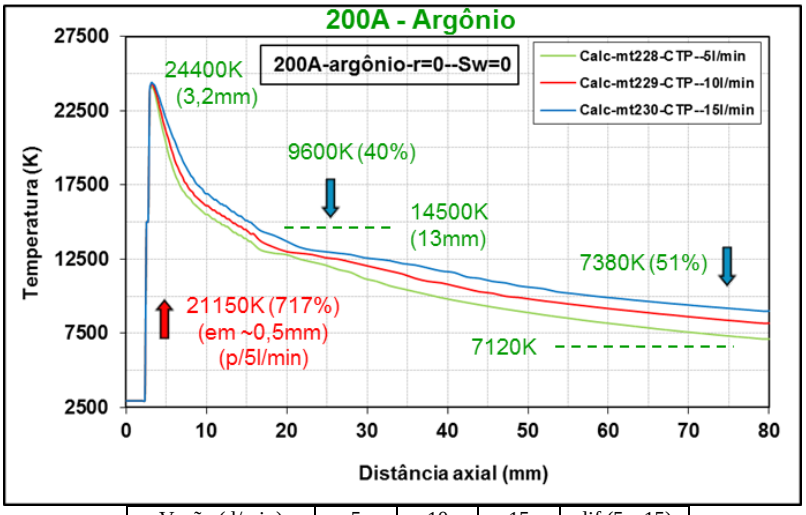

Vazão (l/min)	5	10	15	dif (5 e 15)
Tmax (K) 3,18mm	24100	24300	24400	300K(~1%)
Pos 13mm	14500	15100	15800	1300K(9%)
Pos 80mm	7120	8180	9000	1880(26,4)

Figure 3. Comparison of temperature profiles. Operating conditions: gas: argon; gas flow rate: 5, 10, 15 l/min; electric current intensity: 200A; Sw=0.

The increase in gas-plasma temperature in the area near the cathode end (2,7 to 3,2mm), due to the interaction with the electric arc, is approximately 717% (24400K) to all flow rates, and the difference between the maximum temperatures of the lowest and highest flow is 300K (~1%) (maximum temperature equals to 24400K for 15 l/min and 24100K for 5 l/min). Still within the torch, between 3,2 and 13mm, due to forced and continuous anode cooling, there is a sharp temperature drop (~9600K or ~40%) and at the output of the torch (13mm), the temperature difference between the flow rates of 5 l/min and 15 l/min is 1300K (9%) (temperature is 14500K for 5 l/min and 15800K for 15 l/min). The

free plasma jet, which exchanges heat by convection with the argon environment, presents a less severe temperature decrease (~7380K or ~51%; from 13 to 80mm). However, the temperature difference between the flow rates of 5 and 15 l/min significantly increases in free jet region and it is 26,4% at the end of the computational domain (axial position: 80mm).

Figure 4 shows the comparison among the axial velocity profiles for the argon flow rates of 5, 10 and 15 l/min. It is possible to check that except in gas-plasma acceleration region (region of interaction with the electric arc), the axial velocity is significantly affected by the flow rate. The difference between the maximum axial velocities for 5 and 15 l/min is 42,4% (86m/s). At the end of the torch (13mm), the difference of axial velocity for 5 and 15 l/min is 46% (90m/s) and for the free plasma jet, at the end of the computational domain (80mm), the difference is 132% (57,5m/s).

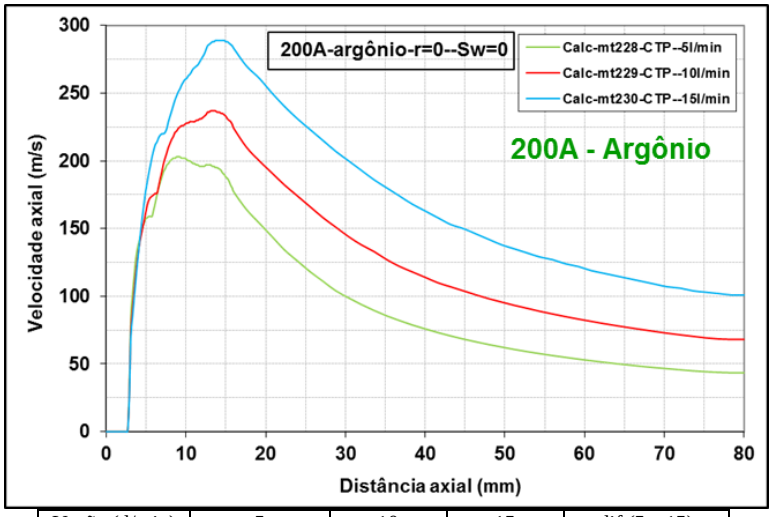

Vazão (l/min)	5	10	15	dif (5 e 15)
Vax max(m/s)	203 (8,8mm)	237 (13,1)	289 (13,7)	86m/s (42,4%)
Pos 13mm	197	237	287	90m/s (46%)
Pos 80mm	43,5	68	101	57,5m/s (132%)

Figure 4. Comparison of axial velocity profiles. Operating conditions: gas: argon; gas flow rate: 5, 10, 15 l/min; electric current intensity: 200A; Sw=0.

3.2 Case 2 - Electric current intensities: 100A and 200A

Figure 5 shows the comparisons of temperature profiles for different electric current intensities (100A and 200A).

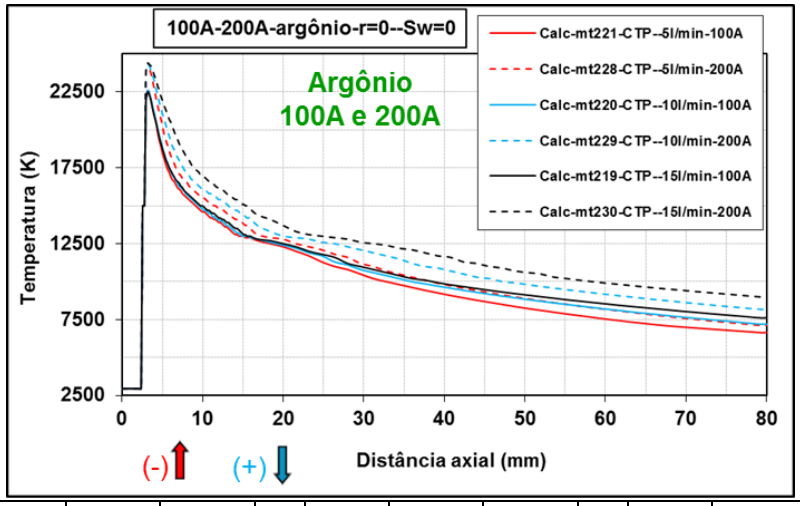

3,2mm	5l/min	10l/min	15l/min	13	5l/min	10l/min	15l/min	80	5l/min	10l/min	15l/min
100A	22600	22600	22500		13600	13700	13900		6650	7210	7620
200A	24100	24300	24400		14500	15100	15800		7120	8180	9000
dif(%)	-6,6%	-7,5%	-8,4%		-6,6	-10,2	-13,7		-7,1	-13,5	-18,1

Figure 5. Comparison of temperature profiles. Operating conditions: gas: argon; gas flow rate: 5, 10, 15 l/min; electric current intensities: 100A and 200A; Sw=0.

The comparisons in Fig. 5 reveal that the temperature profiles for all operating conditions (flow rates and electric current intensities) are very similar in quality.

The maximum temperature obtained with the electric current of 100A (average value for three flow rates: ~22500K; average increase of ~660%) is approximately 7,5% lower than the one obtained with 200A (~24200K ; average increase of ~700%), in the region next to the cathode tip (axial distance: 2,7 to 3,2mm).

In the axial distance of 13mm (end of the torch), the temperature for 100A (~13600K) is approximately 10% lower for 200A (~14500K ; also refer to Fig.3).

In the axial distance of 80mm (end of the computational domain), the temperature for 100A (~6650K) is approximately 13% lower for 200A (~7100K; also refer to Fig. 3).

It is also worth highlighting that the percentage decrease of the maximum temperature by the end of the torch (13mm) is the same for 100A and 200A: 40% (9000K for 100A and 9600K for 200A ; also refer to Fig. 3 – 200A).

The gradual temperature decrease of the free plasma jet, which exchanges heat by convection with the environment gas (argon) in an axial stretch of 13mm to 80mm, is also, in percentage terms, the same for 100A and 200A: 51% (7000K for 100A and 7380K for 200A ; also refer to Fig. 3 – 200A).

As for the temperature profiles, the qualitative similarity between the axial velocity profiles is also checked through Fig. 6.

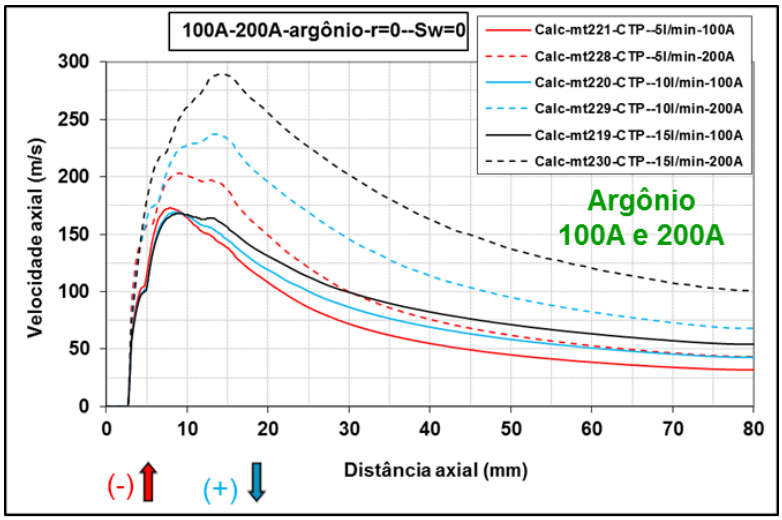

	5l/min	10l/min	15l/min	13	5	10	15	80	5	10	15
100A	173(7,8)	169(8,2)	168(8,6)		148	155	164		32	42,9	54,2
200A	203(8,8)	237(13,1)	289(13,7)		197	237	287		43,5	68,1	101
dif(%)	-17,3%	-40,2%	-72%		-33,1	-52,9	-75		-35,9	-58,7	-86,3

Figure 6. Comparison of axial velocity profiles. Operating conditions: gas: argon; gas flow rate: 5, 10, 15 l/min; electric current intensities: 100A and 200A; Sw=0.

The maximum axial velocities for 100A (5, 10 and 15 l/min) are lower in comparison to the ones for 200A and the percentage differences are 17,3% (5 l/min), 40,2% (10 l/min) and 72% (15 l/min) respectively.

At the end of the torch (13mm), the differences of velocity for 100A and 200A are 33,1% (5 l/min), 52,9% (10 l/min) and 75% (15 l/min).

At the end of the computational domain (80mm), the following differences were obtained: 35,9% (5 l/min), 58,7% (10 l/min) and 86,3% (15 l/min).

3.3 Case 3 - Plasmogenic gases: argon and air

In Fig. 7 and 8 there is a comparison of differences in temperature and axial velocity profiles, respectively, obtained through simulation of plasmogenic gases, argon and air. The torch simulations were performed under the following operating conditions: gas flow rates of 5, 10 and 15 l/min; electric current intensity of 200A.

Analysis of Fig. 7: for the three simulated flow rates, the increase in argon temperature in the arc region, next to the cathode (between 2,7mm and 3,2mm), results in maximum values higher than the ones obtained by the air (between 2,7mm and 3,4mm).

The percentage differences of argon maximum temperatures related to the air are: 12% (5 l/min), 12,3% (10 l/min) and 12,3% (15 l/min). Therefore, taking the average of values related to the three flow rates into consideration, argon presents maximum temperature (~24260K) approximately 12,1% higher than the air (~21300K). Argon and air temperature profiles are very close inside the torch, in the stretch between the axial distances of 8mm and 13mm

(~15000K). The average percentage difference of the three flow rates at the output of the torch (13mm) is 1,7% (higher for argon than for the air). Between the axial distances of 13mm and 35mm (free plasma jet), the temperature decrease of air for the three flow rates is much bigger than the temperature decrease of argon. Between 35mm and the end of the computational domain (80mm), the temperature decrease of air for the three flow rates is less sharp than the temperature decrease of argon. In this stretch, the argon temperature profiles are close to the air, except the air temperature profile of the flow rate of 5 l/min, which has a new sharp drop from the axial distance of 56mm. In axial position 80mm (end of the torch), the percentage differences of argon temperatures related to the air are 21,8% (10 l/min) and 29% (15 l/min). Therefore, taking into consideration the average of values related to the flow rates of 10 l/min and 15 l/min, argon presents temperature (~8600K) approximately 25,4% higher than air (~6390K).

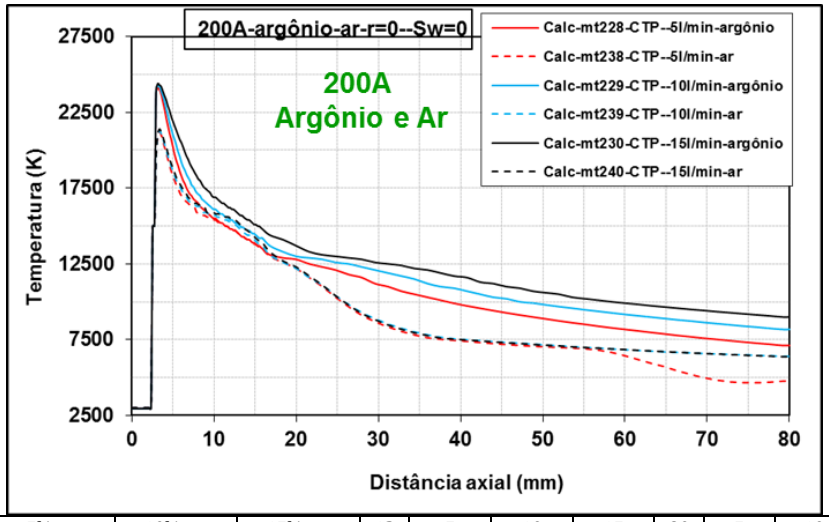

	5l/min	10l/min	15l/min	13	5	10	15	80	5	10	15
argon	24100(3,2)	24300(3,2)	24400(3,2)		14500	15100	15800		7120	8180	9000
ar	21200(3,4)	21300(3,4)	21400(3,4)		14500	14900	15200		4770	6400	6380
dif(%)	+12%	+12,3%	+12,3%		0	+1,3	+3,8		+33	+21,8	+29

Figure 7. Comparison of temperature profiles. Operating conditions: gases: argon and air; gas flow rate: 5, 10, 15 l/min; electric current intensity: 200A; Sw=0.

Figure 8 shows the comparisons of axial velocity profiles for plasmogenic gases: argon and air.

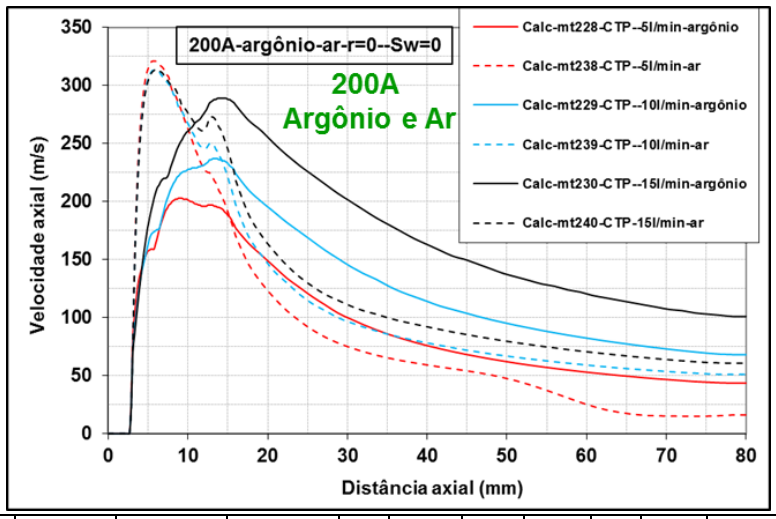

	5l/min	10l/min	15l/min	13	5	10	15	80	5	10	15
argon	203(8,8)	237(13,1)	289(13,7)		197	237	287		43,5	68,1	101
ar	321(5,5)	313(5,5)	314(6)		221	249	273		16,1	51	60,7
dif(%)	-58,1%	-32,1%	-8,7%		-12,2	-5,1	+4,9		+63	+25,1	+40

Figure 8. Comparison of axial velocity profiles. Operating conditions: gases: argon and air; gas flow rate: 5, 10, 15 l/min; electric current intensity: 200A; Sw=0.

Analysis of Fig. 8: concerning the axial velocity profiles for argon and air, there is an inversion in behavior, that is: while the maximum temperatures of the three profiles (three flow rates) related to argon are higher than the ones related to air, the axial velocities of the three profiles (three flow rates) related to air are higher than the ones related to argon.

The percentage differences between the maximum axial velocities for argon and air are - 58,1% (5 l/min), - 32,1% (10 l/min) and - 8,7% (15 l/min). Therefore, taking the average of values related to the three flow rates into consideration, argon has the maximum axial velocity (~243m/s; in ~11,9mm) approximately - 33% lower than air (~316 m/s; in ~5,7mm).

Remarks:

- While the increase in gas-plasma temperature due to *Joule* heating is almost exponentially for both argon (between 2,7mm and 3,2mm, i.e., 0,5mm in axial distance) and air (between 2,7mm and 3,4mm, i.e., 0,7mm), the increase of gas-plasma axial velocity, due to the acceleration caused by the axial component of the *Lorentz* force vector and by the gas-plasma expansion, occurs within an average axial distance of 9,2mm (between 2,7mm and 11,9mm) for argon and within an average axial distance of 3mm (between 2,7mm and 5,7mm) for air.

- As seen by Fig. 8, the maximum axial velocities obtained with the air are not significantly affected by the variation of the flow rate. However, for argon (Fig. 4 and 8), the maximum axial velocity suffers significant effect of flow rate variation: 203m/s (5 l/min), 237m/s (10 l/min) and 289m/s (15 l/min).

- Inside the torch and in the free jet (Fig. 8), the air axial velocity profiles decrease sharply. From the axial distance ~ 20mm, all profiles of argon axial velocity have higher values than the air ones. In axial distance of 80mm (end of the computational domain), the percentage differences between the axial velocity values of argon and air are: 25,1% (10 l/min) and 40% (15 l/min).

4. CONCLUSION

The results obtained with the simulations for case studies, which were performed with the *CTP* code, showed the effects of different operating conditions in plasma flow and, although there are no experimental values for comparisons, physical behaviors and their respective numerical values are consistent with the ones expected in most regions (in relation to the order of magnitude of the numerical results of other studies). Therefore, the *CPT* code proves to be appropriate for the expected purposes, that is, a useful tool to help the development of plasma torch designs.

5. ACKNOWLEDGEMENTS

The authors acknowledge the support from Centro de Pesquisa da Universidade São Judas Tadeu and Escola Politécnica da Universidade de São Paulo.

6. REFERENCES

Abdulkarim, B. I. and Mohd Ariffin Abu Hassan, M. A. A., 2015. "Thermal Plasma Treatment of Wastes: A Review" Australian Journal of Basic and Applied Sciences, 9(31), p: 322-333.

Bauchire, J. M., Gonzalez, J.J. and Gleizes, A., 1997. "Modeling of a DC plasma torch in laminar and turbulent flow", Plasma Chem. Plasma Process., 17,4, pp. 409-432.

Baudry, C., 2003. "Contribution à la modélisation instationnaire et tridimensionnelle du comportement dynamique de l'arc dans une torche de projection plasma",Thèse pour obtenir le grade de Docteur, Universite de Limoges, France.

Bianchini, R. C., 2000, "Modelagem e simulação de processos a plasma para tratamento de organo-clorados", Master Dissertation, Universidade de São Paulo, São Paulo, Brazil.

Boulos, M. I., Fauchais, P. and PFENDER, E., 1994. "Thermal plasma: Fundamentals and applications", Vol. 1, Plenum Press, New York, USA.

Dilawari, A. H., Szekely, J., Batdorf, J., Detering, R. and Shaw, C. B., 1990. "The temperature profiles in an argon plasma issuing into an argon atmosphere: A comparison of measurements and predictions". Plasma Chem. Plasma Process., 10, 2, pp. 321-337.

Fauchais, P., 2004. "Understanding plasma spraying". Journal of Physics D: Applied Physics, 37(9), R86.

Fauchais, P., & Vardelle, A., 2000. "Pending problems in thermal plasmas and actual development". Plasma Physics and Controlled Fusion, 42(12B), B365.

Favalli, R. C., 1997. "Simulação de Tochas de Plasma de Arco Não Transferido", Mater Dissertation, Universidade de São Paulo, São Paulo, Brazil.

Feinman, J., 1987. "Plasma technology in metallurgical processing", Feinman and Associates, USA.

Felipini, C. L., 2015. "Estudo do comportamento do escoamento em tochas de plasma térmico através de simulação numérica". PhD Thesis, Universidade de São Paulo, São Paulo, Brazil.

Felipini, C. L., & Pimenta, M. M., 2015. "Some numerical simulation results of swirling flow in dc plasma torch". In Journal of Physics: Conference Series (Vol. 591, No. 1, p. 012038). IOP Publishing.

Gleizes, A., Gonzalez, J. J. and Freton, P., 2005. "Thermal plasma modeling", J. Phys. D: Appl. Phys., 38, pp.153-183.

Gomez, E., Rani, D. A., Cheeseman, C. R., Deegan, D., Wise, M., & Boccaccini, A. R., 2009. "Thermal plasma technology for the treatment of wastes: a critical review". Journal of Hazardous Materials, 161(2), 614-626.

Heberlein, J., & Murphy, A. B., 2008. "Thermal plasma waste treatment". Journal of Physics D: Applied Physics, 41(5), 053001.

Hsu, K. C., Etemadi, K.and Pfender, E., 1983. "Study of the free-burning high intensity argon arc", J. Appl. Phys., 54, pp. 1293-1301.

Huang, R., Fukanuma, H., Uesugi, Y. and Tanaka, Y., 2013. "Comparisons of Two Models for the Simulation of a DC Arc Plasma Torch", Journal of thermal spray technology", 22(2-3), pp. 183-191.

Klinger, L., 2002. "Simulation numérique 3d d'une torche à plasma par une méthode de volumes finis", Thèse pour obtenir le grade de Docteur, L'école Polytechnique de Lausanne, Switzerland.

Li, H. P., Pfender, E. and Chen, X., 2003. "Application of Steenbeck's minimum principle for three-dimensional modeling of dc arc plasma torches", J. Phys. D: Appl. Phys., 36, pp. 1084-1096.

Li, H. P. and Pfender, E., 2007. "Three dimensional modeling of the plasma spray process", Journal of Thermal Spray Technology, 6(2), pp. 245-260.

Mihovsky, M., 2010. "Thermal plasma application in metallurgy". Journal of the University of Chemical Technology and Metallurgy, 45(1), 3-18.

Murphy, A B. and Kovitya , P., 1993. "Mathematical model and laser-scattering temperature measurements of a direct-current plasma torch discharging into air", J. Appl. Phys.,15, pp.4759.

Pfender, E., 1978. "Electric arcs and arc gas heaters". Gaseous electronics, 1(5), 291-298.

Pfender, L.F., 2000. "Trends in Thermal Plasma Technology". Thermal Plasma Torches and Technologies. 1: 20-41.

Rao, L., Rivard, F., & Carabin, P., 2013. "Thermal plasma torches for metallurgical applications". In 4th International Symposium on High-Temperature Metallurgical Processing (pp. 57-65). John Wiley & Sons, Inc..

Scott, D. A., Kovitya, P. and Haddad, G. N., 1989. "Temperatures in the plume of a dc plasma torch", J. Appl. Phys., 66, pp. 5232.

Solonenko, O. P. and Zhukov, M. F., 1995. Thermal Plasma and New Materials Technology, Cambridge Interscience Publishing, Cambridge, 1995.

Trelles, J. P., Chazelas, C., Vardelle, A. and Heberlein, J. V. R., 2009. "Arc plasma torch modeling", Journal of Thermal Spray Technology, 18(5-6), pp. 728-752.

Vardelle, A., Moreau, C., Themelis, N. J., & Chazelas, C., 2015. "A perspective on plasma spray technology". Plasma Chemistry and Plasma Processing, 35(3), 491-509.

Vatavuk, P., 1996. "Convecção Natural Transitória no Interior de um Recipiente Cilíndrico Vertical", PhD Thesis, Universidade de São Paulo, São Paulo, Brazil.

Venkatramani, N., 2002. "Industrial plasma torches and applications". CURRENT SCIENCE-BANGALORE-, 83(3), 254-262.

Westhoff, R. and Szekely, J., 1991. "Model of fluid, heat flow, and electromagnetic pheomena in a nontransferred arc plasma torch", J. Appl. Phys., Vol. 70, pp. 3455-3466.

Yuan, X. Q., Li, H., Zhao, T. Z., Wang, F., Guo, W. K., and Xu, P., 2004. "Comparative study of flow characteristics inside plasma torch with different nozzle configurations", Plasma Chem. Plasma Process., 24(4), pp. 585-601.

7. RESPONSIBILITY NOTICE

The authors are the only responsible for the printed material included in this paper.